

LETTERS

Sodium salts in E-ring ice grains from an ocean below the surface of Enceladus

F. Postberg^{1,2}, S. Kempf^{2,3}, J. Schmidt⁴, N. Brilliantov^{5,6}, A. Beinsen⁷, B. Abel^{7,8}, U. Buck⁹ & R. Srama²

Saturn's moon Enceladus emits plumes of water vapour and ice particles from fractures near its south pole^{1–5}, suggesting the possibility of a subsurface ocean^{5–7}. These plume particles are the dominant source of Saturn's E ring^{7,8}. A previous *in situ* analysis⁹ of these particles concluded that the minor organic or siliceous components, identified in many ice grains, could be evidence for interaction between Enceladus' rocky core and liquid water^{9,10}. It was not clear, however, whether the liquid is still present today or whether it has frozen. Here we report the identification of a population of E-ring grains that are rich in sodium salts (~0.5–2% by mass), which can arise only if the plumes originate from liquid water. The abundance of various salt components in these particles, as well as the inferred basic pH, exhibit a compelling similarity to the predicted composition of a subsurface Enceladus ocean in contact with its rock core¹¹. The plume vapour is expected to be free of atomic sodium. Thus, the absence of sodium from optical spectra¹² is in good agreement with our results. In the E ring the upper limit for spectroscopy¹² is insufficiently sensitive to detect the concentrations we found.

The compositional *in situ* analysis of E-ring grains provides unique information about the composition of plume material combined with otherwise unachievable detection statistics. The Cosmic Dust Analyser¹³ (CDA) aboard the Cassini spacecraft recorded thousands of mass spectra of E-ring particles, predominantly with radii of 0.1–1 μm . The instrument's chemical analyser subsystem produces time-of-flight mass spectra of cations and cationic aggregates of the gas and plasma cloud generated by high-velocity impacts of single grains onto a metal target.

Previous CDA results show that the bulk material of E-ring particles is water ice^{9,14}. There appear to be distinct families of spectra, types I and II of which have already been introduced in previous work⁹. Type I spectra imply almost pure water ice; type II spectra exhibit significant amounts of organic and/or siliceous material. These non-water components alone imply the past or present interaction of liquid water with a rocky Enceladian core⁹.

Sodium is considered the perfect indicator for a still existing liquid¹¹. In the case of a slow downward freezing, as would be expected for icy planetary bodies, sodium salts previously dissolved from rock remain in the liquid phase, so the ice crust is expected to be almost salt-free¹¹. Therefore, sublimation from heated water ice¹⁵ or clathrate decomposition¹⁶ in the crust cannot generate the measured Na concentrations. The detection of sodium in Enceladus' plume material is only plausible for a liquid source.

Approximately 93% of the E-ring spectra in the evaluated data set, obtained between October 2004 and December 2005 (Supplementary Information), show a Na⁺ mass line and/or cluster (aggregate) ions

containing Na⁺ (Fig. 1). Cluster formation occurs during the impact and is very sensitive to the Na/H₂O ratio¹⁷, providing a method of constraining the Na concentrations of the ice particles (Fig. 1).

About 6% of these spectra (hereafter 'type III' spectra) show a unique mass line pattern which we now attribute to ice particles with particularly high sodium contents (Fig. 1b). In addition to water and sodium they exhibit features that indicate the sodium salts NaCl, NaHCO₃ and/or Na₂CO₃ as significant constituents. Weaker K⁺ mass lines suggest a minor contribution from potassium salts. On average, K⁺ is 100 to 200 times less abundant than Na⁺. The majority of E-ring ice spectra are of types I and II⁹. Na features are identified in over 90% of these spectra (a substantially higher percentage than found in the previous analysis, which considered only the most prominent mass lines⁹), albeit at much lower abundances than in the type III population (Fig. 1a).

In previous work, the Na⁺ mass lines of Na-poor type I and II spectra were tentatively attributed to Na-bearing compounds having contaminated the detector's target before Cassini's launch^{9,14}. However, the concentration of salts indicated by type III spectra is above any possible level of target contamination¹⁸. Furthermore, contamination as a dominant origin of the frequent low-abundance Na⁺ mass lines in type I and II spectra can also be ruled out, because a careful analysis¹⁸ significantly restricts the possible degree of Na contamination (Supplementary Information).

To constrain our interpretation further, we have recorded mass spectra of water aggregates generated from a laser-dispersed liquid¹⁹ from a solution with different sodium salt concentrations (Supplementary Information). All Na-rich type III spectra mass lines (Fig. 1b) are reproduced well by laboratory spectra (Fig. 2b) from a NaCl/NaHCO₃ solution with 0.05–0.2 mol kg⁻¹ NaCl and 2–5 times more NaCl than NaHCO₃. To reproduce the Na-poor E-ring spectra (Fig. 1a), very dilute salt solutions (Na/H₂O < 10⁻⁷) are required (Fig. 2a). This implies at least two populations of ice grains, whose Na content differs by more than four orders of magnitude. Spectra with intermediate Na-concentrations are rare (<3%).

We suggest that the Na-rich grains are directly frozen submicrometre-sized droplets from the liquid plume reservoir. We employ a liquid dispersion model^{19,20}, assuming that—above the salt solution— aerosol-like droplets are produced (Fig. 3a), possibly by ascending bubbles of plume gases⁴ (CO₂, N₂, CO, CH₄) in the liquid or by other processes that can disperse the liquid under the given conditions.

Another effective mechanism for grain formation is direct condensation of the ascending vapour within the ice channels⁷. The low Na content of type I and II grains (which amount to more than 90% of the recorded spectra) might thus directly reflect the low concentration of NaCl molecules in the water vapour above the liquid (Fig. 3b).

¹Institut für Geowissenschaften, Universität Heidelberg, 69120 Heidelberg, Germany. ²Max-Planck-Institut für Kernphysik, 69117 Heidelberg, Germany. ³IGEP, Technische Universität Braunschweig, 38106 Braunschweig, Germany. ⁴Nichtlineare Dynamik, Universität Potsdam, 14476 Potsdam-Golm, Germany. ⁵Department of Mathematics, University of Leicester, Leicester LE1 7RH, UK. ⁶Department of Physics, Moscow State University, 119991 Moscow, Russia. ⁷Institut für Physikalische Chemie, Universität Göttingen, 37077 Göttingen, Germany. ⁸Wilhelm-Oswald-Institut für Physikalische und Theoretische Chemie, Universität Leipzig, 04103 Leipzig, Germany. ⁹Max-Planck-Institut für Dynamik und Selbstorganisation, 37073 Göttingen, Germany.

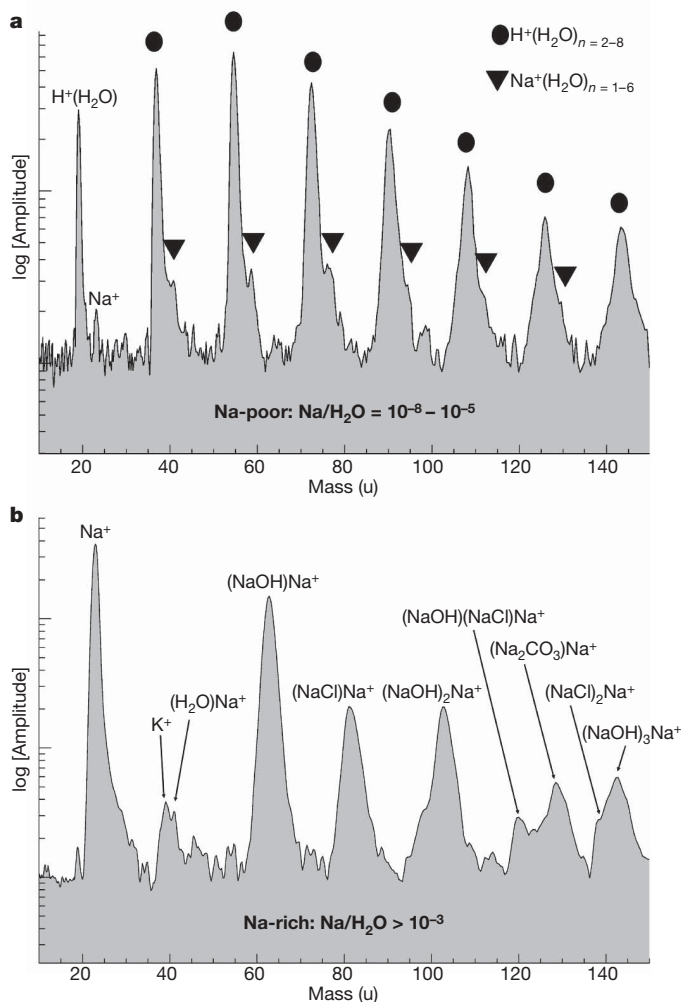


Figure 1 | Spectra of E-ring particles with differing Na/H₂O ratio.

a, Spectrum of a Na-poor ice particle (types I and II), dominated by a sequence of water cluster ions of the form $\text{H}(\text{H}_2\text{O})_n^+$, ($n = 2-8$). Weak mass lines of Na^+ and Na-hydrate ions ($\text{Na}(\text{H}_2\text{O})_n^+$) are also present. The sensitivity of the detector to Na is at least several hundred times higher than to water, so the respective ice grains contain only traces of sodium. From the peak amplitudes we infer a varying Na/H₂O mixing ratio within the Na-poor ice grains (types I and II) of $5 \times 10^{-5(\pm 1)}$ to $5 \times 10^{-8(\pm 1)}$ (Supplementary Information). Often K^+ (39u, where u means unified atomic mass units, or daltons) and its respective hydrates— $\text{K}(\text{H}_2\text{O})_n^+$ —are also detectable. However, reliable determinations of the K concentrations have not been obtained, owing to overlapping of K spectral features with abundant water and Na-cluster mass lines. **b**, Co-added spectra of Na-rich water-ice particles (type III). Although the particles are still predominantly water, these spectra typically show very few pure water and Na-hydrate clusters, if any. They are characterized by an abundant Na^+ mass line followed by a peak sequence of hydroxyl-cluster-ions $\text{Na}(\text{NaOH})_n^+$, representing the defining pattern of a type III spectrum. Laboratory experiments (Fig. 2) confirm that this cluster type is dominant only if the Na/H₂O ratio exceeds 10^{-3} . The pronounced appearance of $\text{Na}(\text{NaOH})_n$ signatures also indicate an alkaline liquid. In addition, these spectra often show $\text{Na}(\text{NaCl})_n^+$, (where $n = 1-3$), and $\text{Na}(\text{Na}_2\text{CO}_3)^+$, which implies that NaCl followed by NaHCO_3 and/or Na_2CO_3 are the main Na-bearing compounds (also Fig. 2 and Supplementary Information). A small amount of K^+ is also present. These are exactly the four most-abundant non-water species predicted to exist in an ocean within Enceladus¹¹.

Thermodynamically, a highly depleted NaCl gas phase in equilibrium with non-dissociated NaCl in the liquid¹¹ is in fact expected (Fig. 4 and Supplementary Information). A fraction of Na-free type I grains might also be ejecta from the surface of Enceladus, caused by micro-meteoroid impacts⁹.

For an ocean in equilibrium with a rocky Enceladus core, Na^+ concentrations of $0.05-0.1 \text{ mol kg}^{-1}$, an overall salinity of

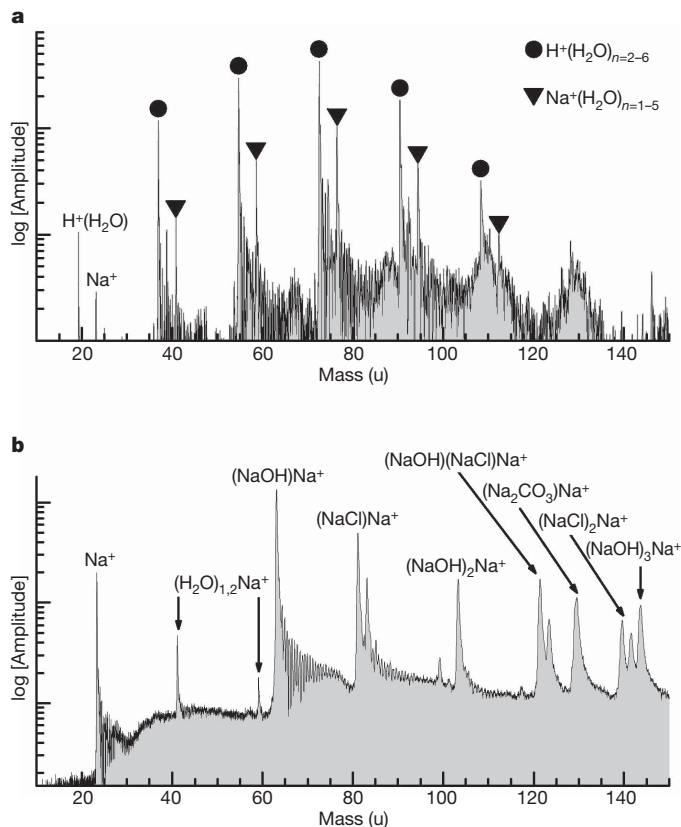


Figure 2 | Reproduction of CDA measurements in the laboratory by laser dispersion¹⁹ of salt water. Differences between the laboratory experiments (laser shot on a liquid) and CDA (high-speed impact of an ice grain), have no effect on our interpretation (Supplementary Information). What is important is that both measurements, in the laboratory and at Enceladus, start from a similar liquid solution. **a**, Cation spectrum of water with $10^{-6} \text{ mol kg}^{-1} \text{ NaCl}$ ($\text{Na}/\text{H}_2\text{O} \approx 2 \times 10^{-8}$). It shows the same cluster characteristics as Na-poor (types I and II) E-ring grains (Fig. 1a). $\text{H}(\text{H}_2\text{O})_n^+$ clusters dominate but Na^+ and its hydrates— $\text{Na}(\text{H}_2\text{O})_n^+$ —are also present. The NaCl concentration of Na-poor spectra inferred from the laboratory experiments is at the lower boundary of our earlier estimates (Fig. 1a). **b**, Ion spectrum of water with $0.2 \text{ mol kg}^{-1} \text{ NaCl}$ and $0.1 \text{ mol kg}^{-1} \text{ NaHCO}_3$ ($\text{Na}/\text{H}_2\text{O} \approx 5 \times 10^{-3}$, $\text{pH} = 9$). Except for the better resolution, all characteristic mass lines are identical to a Na-rich (type III) E-ring grain spectrum (Fig. 1b): few Na-hydrates but abundant $\text{Na}(\text{NaOH})_n^+$, $\text{Na}(\text{NaCl})_n^+$ and $\text{Na}(\text{Na}_2\text{CO}_3)^+$ clusters are observed. The cluster pattern not only allows for estimates of the NaCl, NaHCO_3 and KCl content, but also of the pH of a liquid solution with the ice grain composition.

$3-8 \text{ g kg}^{-1}$, and an alkaline pH of 8–11 have been predicted¹¹. The increasing proportion of salts within the remaining liquid phase, caused by slow downward freezing of an early ocean, has also been quantified¹¹. Using the correlation between laboratory experiments and CDA spectra, we find that the composition of type III E-ring grains agrees with the modelled Enceladus ocean composition. Our values for the concentrations of NaCl ($0.05-0.2 \text{ mol kg}^{-1}$) and the Na-carbonates ($0.02-0.1 \text{ mol kg}^{-1}$) as well as the inferred alkalinity (pH 8.5–9) match the model. However, the Na/K ratio is about ten times higher than predicted¹¹. This may be due to K-deposition in clays at the rock-water interface, a process well known from terrestrial waters²¹. Our measurements imply a ‘soda-ocean’ rich in bicarbonate and/or carbonate. This is consistent with the abundant CO_2 observed in the plume vapour⁴. Escaping gases⁴ are probably also generated by clathrate decomposition at the water–ice boundary or hydrothermal processes¹⁰. Alkaline salt water, together with the observed organic compounds^{4,9} and the thermal energy obviously present in the south polar region⁶, could provide an environment well suited for the formation of life precursors^{22,23}.

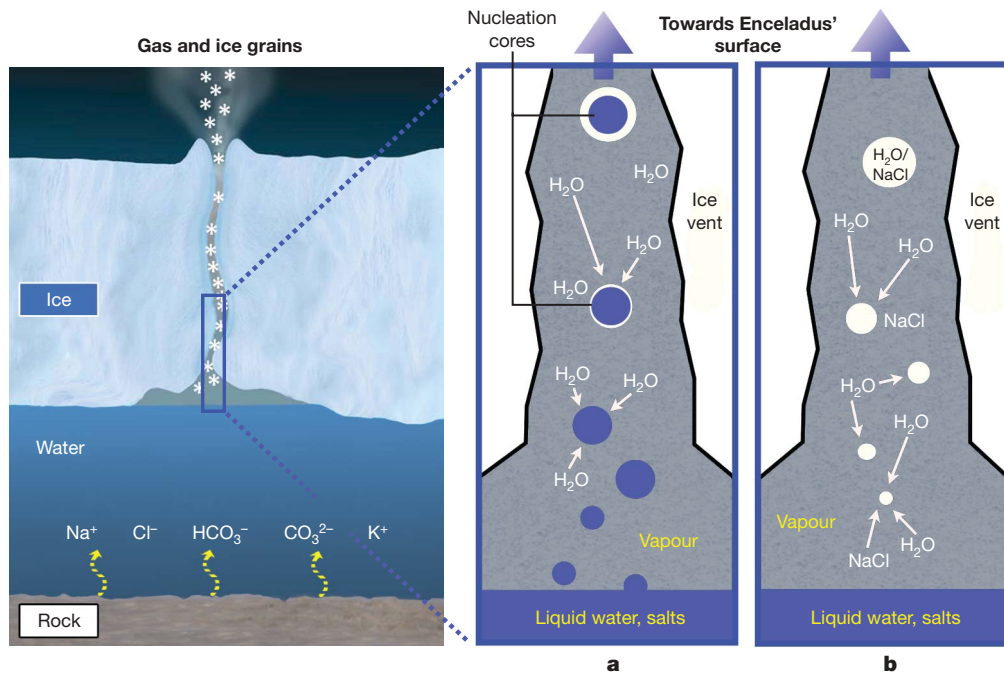


Figure 3 | Schematic of how liquid dispersion and condensation from vapour form ice particles with very different Na content. **a**, Na-rich grains. Aerosol-like droplets (blue) are generated by dispersion above the salty liquid. They preserve the ocean's composition. Such droplets (submicrometre- to micrometre-sized) would condense some additional water from the supersaturated gas⁷ that drags them towards the surface. Therefore, the salt content of Na-rich (type III) grains can be considered a lower limit for the

Individual plume sources stay active for years²⁴, implying outflow from a large reservoir. Moreover, given the observed gas production rate² ($\sim 150\text{--}300\text{ kg s}^{-1}$), it can be shown (using heat-flow arguments)

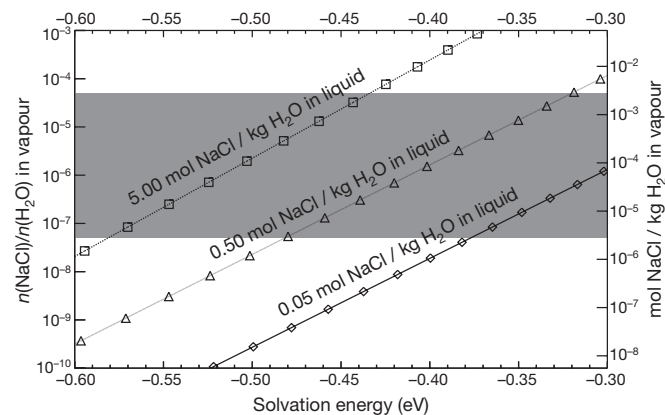


Figure 4 | Equilibrium concentrations of NaCl in the vapour phase above a subsurface Enceladus water reservoir. The calculated NaCl vapour concentration (Supplementary Information) is plotted for the case of a slightly salty ocean (0.05 mol kg^{-1} , diamonds), an earth-like ocean (0.5 mol kg^{-1} , triangles) and a NaCl brine close to the eutectic concentration (5 mol kg^{-1} , squares). The dissolved ions, Na^+ and Cl^- , cannot evaporate owing to their high solvation energy, so the concentration of NaCl in the vapour depends on the solvation energy of the small fraction of undissociated NaCl dipoles existing in the liquid. We constrained the range of plausible solvation energies to $0.3\text{--}0.6\text{ eV}$ per molecule (Supplementary Information). The grey area shows the Na concentration inferred for Na-poor (types I and II) E-ring particles. For a wide range of plausible solvation energies and NaCl molalities in the ocean, the measured Na content is in agreement with that of vapour evaporated from a salty ocean. The initially low vapour concentration of molecular alkali compounds is probably further depleted by the higher condensation rates of such refractory compounds (for example, at the crack walls).

surface of an Enceladus ocean. **b**, Na-poor grains. The standard formation of ice grains by condensation of water vapour ascending from the liquid reservoir with subsequent growth and transport in the vent⁷. The particles initially have the same low ratio of $\text{Na}/\text{H}_2\text{O}$ as the gas (Fig. 4). By direct or indirect interaction (such as via crack walls) with the Na-rich grains, they may be further enriched with Na-salt traces. Therefore, the salt content of the Na-poor grains can be considered an upper limit for that of the plume gas.

that the area of the liquid–gas interface must be at least of the order of square kilometres (Supplementary Information). This requires large vapour chambers above the liquid that narrow to the vent channels. A local enhancement of salinity (owing to evaporation) will be rapidly mixed with the bulk of the liquid. The salt-enrichment of the reservoir is a slow process, not violating the steady-state assumption for vent dynamics⁷. For example, the timescale for evaporation (and increasing salinity) even for an isolated liquid reservoir of an equivalent radius of 10 km would be $300,000\text{ years}$ (Supplementary Information).

So far, no atomic Na or K has been detected in Enceladus' environment by spectroscopy¹². This does not contradict our results. The sodium in the plumes is almost entirely located in the type III grains. On a very low level, dissolved alkali salts (NaCl and KCl) evaporate only in molecular (not atomic) form (Fig. 4 and Supplementary Information). Moreover, any free alkali atoms will quickly react in a water vapour environment^{25–27}. However, particles are subject to plasma sputtering in the E ring and over decades embedded alkali compounds will be slowly released from the grains. The current detection limit for optical Na emission in E-ring gas is equivalent to a $\text{Na}/\text{H}_2\text{O}$ mixing ratio¹² of 7×10^{-6} . Making the (simplified) assumption of similar particle masses in Na-rich and Na-poor populations, the average $\text{Na}/\text{H}_2\text{O}$ ratio (types I, II and III) in E-ring ice grains is estimated to be 3×10^{-4} to 3×10^{-5} . However, most of the total ejected grain mass falls back to the moon's surface^{7,28} (the cryo-volcanically active regions should be covered with Na-bearing plume particles), so the particle total mass ejected into the E ring is about 200 times less than the mass of water vapour^{2,5}. Therefore, the overall $\text{Na}/\text{H}_2\text{O}$ E-ring mixing ratio is diluted to roughly $10^{-6}\text{--}10^{-7}$, significantly below the optical detection limit.

Received 4 September 2008; accepted 6 April 2009.

- Dougherty, M. K. *et al.* Identification of a dynamic atmosphere at Enceladus with the Cassini magnetometer. *Science* **311**, 1406–1409 (2006).
- Hansen, C. J. *et al.* Enceladus' water vapor plume. *Science* **311**, 1422–1425 (2006).
- Spahn, F. *et al.* Cassini dust measurements at Enceladus and implications for the origin of the E ring. *Science* **311**, 1416–1418 (2006).

4. Waite, J. H. *et al.* Cassini ion and neutral mass spectrometer: Enceladus plume composition and structure. *Science* **311**, 1419–1422 (2006).
5. Porco, C. C. *et al.* Cassini observes the active south pole of Enceladus. *Science* **311**, 1393–1401 (2006).
6. Spencer, J. R. *et al.* Cassini encounters Enceladus: background and the discovery of a south polar hot spot. *Science* **311**, 1401–1405 (2006).
7. Schmidt, J., Brilliantov, N., Spahn, F. & Kempf, S. Slow dust in Enceladus' plume from condensation and wall collisions in tiger stripe fractures. *Nature* **451**, 685–688 (2008).
8. Kempf, S. *et al.* The E ring in the vicinity of Enceladus. I. Spatial distribution and properties of the ring particles. *Icarus* **193**, 420–437 (2008).
9. Postberg, F. *et al.* The E ring in the vicinity of Enceladus. II. Probing the moon's interior—the composition of E-ring particles. *Icarus* **193**, 438–454 (2008).
10. Matson, D. L., Castillo, J. C., Lunine, J. & Johnson, T. V. Enceladus' plume: compositional evidence for a hot interior. *Icarus* **187**, 569–573 (2007).
11. Zolotov, M. Y. An oceanic composition on early and today's Enceladus. *Geophys. Res. Lett.* **34**, L23203 (2007).
12. Schneider, N. M. *et al.* No sodium in the vapour plumes of Enceladus. *Nature* doi:10.1038/nature08070 (this issue).
13. Srama, R. *et al.* The Cassini cosmic dust analyzer. *Space Sci. Rev.* **114**, 465–518 (2004).
14. Hillier, J. K. *et al.* The composition of Saturn's E ring. *Mon. Not. R. Astron. Soc.* **388**, 1588–1596 (2007).
15. Nimmo, F., Spencer, J. R., Pappalardo, R. T. & Mullen, M. E. Shear heating as the origin of the plumes and heat flux on Enceladus. *Nature* **447**, 289–291 (2007).
16. Kieffer, S. W. *et al.* A clathrate reservoir hypothesis for Enceladus' south polar plume. *Science* **314**, 1764–1766 (2006).
17. Steinbach, C. & Buck, U. Reaction and solvation of sodium in hydrogen bonded solvent clusters. *Phys. Chem. Chem. Phys.* **7**, 986–990 (2005).
18. Postberg, F. *et al.* Discriminating contamination from particle components in spectra of Cassini's dust detector CDA. *Planet. Space Sci.* (in the press).
19. Charvat, A. & Abel, B. How to make big molecules fly out of liquid water: applications, features and physics of laser assisted liquid phase dispersion mass spectrometry. *Phys. Chem. Chem. Phys.* **9**, 3335–3360 (2007).
20. Frohn, A. & Roth, N. *Dynamics of Droplets* 245–260 (Springer, 2000).
21. Harder, H. Über das Kalium-Natrium-Verhältnis in Gewässern und die Tonmineralbildung. *Naturwissenschaften* **54**, 613 (1967).
22. Kempe, S. & Kazmierczak, J. Biogenesis and early life on Earth and Europa: favoured by an alkaline ocean? *Astrobiology* **2**, 123–130 (2002).
23. McKay, C. P., Porco, C. C., Altheide, T., Davis, W. L. & Kral, T. A. The possible origin and persistence of life on Enceladus and detection of biomarkers in the plume. *Astrobiology* **8**, 909–919 (2008).
24. Spitale, J. N. & Porco, C. C. Association of jets on Enceladus with the warmest regions on its south-polar fractures. *Nature* **449**, 695–697 (2007).
25. Dzidic, I. & Kebarle, P. Hydration of the alkali ions in the gas phase. *J. Phys. Chem.* **74**, 1466–1474 (1969).
26. Schulz, C. P., Haugstätter, R., Tittes, H. U. & Hertel, I. V. Free sodium-water clusters. *Phys. Rev. Lett.* **57**, 1703–1706 (1986).
27. Buck, U. & Steinbach, C. Formation of sodium hydroxide in multiple sodium-water cluster collisions. *J. Phys. Chem. A* **102**, 7333–7336 (1998).
28. Kempf, S., Beckmann, U. & Schmidt, J. How the Enceladus dust plumes form Saturn's E ring. *Icarus*. (submitted).

Supplementary Information is linked to the online version of the paper at www.nature.com/nature.

Acknowledgements We thank U. Beckmann, M. Burger, M. Burton, M. Gellert, E. Grün, J. K. Hillier, N. Schneider, F. Spahn, and M. Zolotov for discussions. We acknowledge the efforts of the Cassini team and JPL. The work has been supported by the DLR, the DFG and the Frontier programme of the University of Heidelberg.

Author Information Reprints and permissions information is available at www.nature.com/reprints. Correspondence and requests for materials should be addressed to F.P. (frank.postberg@mpi-hd.mpg.de).